Surface Science 603 (2009) 1389–1396

Contents lists available at ScienceDirect

Surface Science

journal homepage: www.elsevier.com/locate/susc

# Quantum oscillations in surface properties

A.L. Vázquez de Parga [a,b], J.J. Hinarejos [b], F. Calleja [b], J. Camarero [a,b], R. Otero [a,b], R. Miranda [a,b,*]

[a] Instituto Madrileño de Estudios Avanzados en Nanociencia, (IMDEA-Nanociencia), Cantoblanco, 28049 Madrid, Spain
[b] Departamento de Física de la Materia, Condensada e Instituto de Ciencia de Materiales N. Cabrera, Universidad Autónoma de Madrid, Cantoblanco, 28049 Madrid, Spain

ARTICLE INFO

*Article history:*
Available online 18 January 2009

*Keywords:*
Quantum size effects
Metallic films
Scanning tunneling microscopy
Scanning tunneling spectroscopy

ABSTRACT

Many properties of metallic thin films have been shown to oscillate with film thickness due to quantum size effects, i.e. the confinement of electrons inside epitaxial metal overlayers which causes quantization of the electronic states. This is a very general phenomenon and it affects both bulk properties of the films, such as resistivity or superconducting transition temperatures, and surface properties, such as chemical reactivity, diffusivity, thermal stability, i.e surface roughening transitions. In this paper we describe some of these thickness-dependent properties which affect the stability of nanostructures and allow us to tailor their properties. We shall concentrate in the paradigmatic example of thin films of Pb grown on metallic and semiconducting substrates and how one can achieve the growth of highly perfect, atomically flat, epitaxial films on different substrates, due to the kinetic constrains imposed by the presence of QSE, a topic increasingly important in the production of nanoscale quantum devices.



## 1. Introduction

Quantum Size Effects (QSE) in ultrathin metal films, where electrons are confined in the perpendicular direction by suitable energy barriers (e.g. band gaps in the substrate and image potential in the vacuum side), lead to *oscillations* in many physical properties upon variation of the film thickness. This is produced by the systematic variation in the Density Of States (DOS) at the Fermi level due to its periodic crossing by the Quantum Well States (QWS) created by the confinement of electrons.

These QSE were first predicted by Sandomirskii more than 40 years ago [1], but it has taken a long time to determine experimentally their existence. In the past few years many bulk properties of thin metallic films have been predicted or observed to oscillate with film thickness, being the periodicity (of few monolayers) dictated by the Fermi surface geometry of the metal. Among them we may mention the electron density inside and outside a metal film [2,3], the film interlayer distances [4], the metallicity [5], the electrical resistivity in tunneling [6,7], the Hall coefficient [8], the superconducting transition temperature [9–11] or the intensity of the electron–phonon coupling [12]. In most of the examples above, the chosen metal was Pb and the oscillations displayed a bilayer periodicity and a superimposed beating period, as dictated by the Fermi surface of bulk Pb.

In what follows we describe the oscillation of a number of surface properties in ultrathin metallic films due to the presence of QSE, from the stabilization of certain (magic) island heights in Stranski-Kastranov films, to the surface roughening temperature, work function, chemical reactivity, or the surface diffusion barrier. These oscillations appear because of a substantial contribution of the QWS to the total energy of the system and the Density of States at the Fermi level, in a manner completely equivalent to the oscillatory magnetic coupling across non-magnetic layers [13], which is revealed in the Giant Magneto Resistance effect [14]. QSE might be of fundamental importance in the search for methods to produce highly organized structures at the atomic scale during epitaxy, an active research area that holds the promise for basic discoveries and technological applications of novel quantum devices. As an example of the latter, we shall show that the crucial role of QSE during epitaxial growth can be employed to stabilize atomically flat, highly reflecting mirrors for He atoms, a crucial ingredient to develop an Scanning Atom Microscope.

Most of the results to be shown in the following correspond to the systems Pb/Cu(1 1 1) and Pb/Si(1 1 1), which have been investigated by Scanning Tunneling Microscopy and Spectroscopy (STM/STS) as well as by a number of spatially averaging techniques. These systems have been chosen because of their peculiar growth mode (almost layer-by-layer when grown at low enough temperature, but Stranski-Kastranov close to Room Temperature (RT)), and electronic structure; electrons from the s–p band of Pb are efficiently confined between the vacuum barrier at the film surface and the electronic gaps at the Pb/Cu or Pb/Si interfaces. Concerning the techniques used, reciprocal space techniques have the weakness of emphasizing the most probable configuration averaging

* Corresponding author. Address: Departamento de Física de la Materia, Condensada e Instituto de Ciencia de Materiales N. Cabrera, Universidad Autónoma de Madrid, Cantoblanco, 28049 Madrid, Spain. Tel.: +34 1 3974737/4758; fax: +34 1 3973961.
*E-mail address:* rodolfo.miranda@uam.es (R. Miranda).

0039-6028/$ - see front matter © 2009 Elsevier B.V. All rights reserved.
doi:10.1016/j.susc.2008.08.039

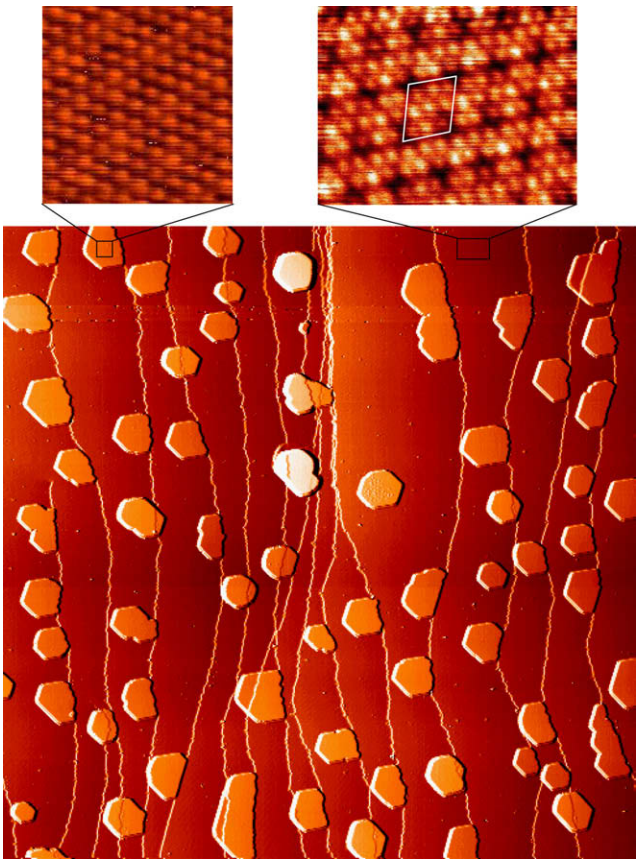

**Fig. 1.** 500 nm × 500 nm STM image of the morphology of 2 ML of Pb deposited on Cu(1 1 1) at 300 K. The insets show atomically resolved images of the 4 × 4 wetting layer (right) and the (1 1 1) face of Pb on top of the crystallites (left).

over lateral length scales difficult to determine precisely; on the other hand, real-space, local techniques such as STM/STS, offer a invaluable insight on these nanosystems, often challenging the view obtained from averaging techniques, as illustrated recently in relation to the thickness dependence of the superconducting temperature for nanometer-thick films of Pb on Si(1 1 1) [11], where a real-space view of the superconducting gap has corrected previous inconsistencies [10].

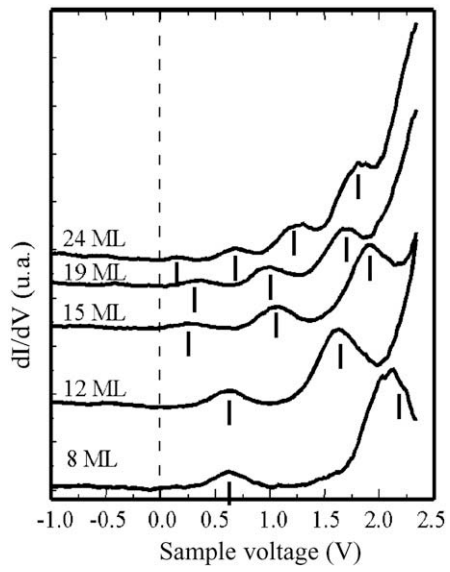


**Fig. 2.** Tunnelling spectra recorded at 300 K on top of Pb(1 1 1) islands of different height.

## 2. Quantum well states in Pb nanostructures

As described above, crossing the Pb/Cu and Pb/Si interfaces is forbidden for electrons at the s–p band in Pb in the (1 1 1) direction. In the case of Si this is due to the presence of a real bandgap of about 1 eV around the Fermi level. In spite of the metallicity of Cu, the situation at the Pb/Cu(1 1 1) interface is very similar, since there exist a directional bandgap around the (1 1 1) direction around the Fermi energy going from −1 to +4 eV. The electrons both in continuous thin Pb films or Pb nanocrystallites are thus confined in the direction perpendicular to the film, leading to the existence of QWS, which can be detected by local Tunneling Spectroscopy [15].

A system that is particularly well suited for this experiment is Pb deposited at RT on Cu(1 1 1). As shown in Fig. 1, Pb grows on Cu(1 1 1) at 300 K in the Stranski-Krastanov mode of growth, whereby 3D, (1 1 1)-oriented Pb islands grow on top of a wetting layer, just 1 ML high [16]. Accordingly, the surface appears covered with 3D islands, most of them of similar height. Only the islands nucleated at step bunches are significantly higher. The inset shows an atomically resolved image of the wetting monolayer of Pb that exists between the islands. This is a compact, hexagonal, Pb monolayer that forms a (4 × 4) superstructure with respect to the Cu(1 1 1) substrate, easily detected also by Low Energy Electron Diffraction [17].

The Stranski-Kastranov growth mode ensures that, not only the electronic structure of the Pb crystallites can be obtained by STS, but also the quantum well width is experimentally accessible as it is given by the height of the islands in the STM images. Fig. 2 shows selected STM spectra recorded on top of islands with different heights. A number of peaks is found is these spectra, whose energy positions vary with island height (well width), as expected for QWS. The robustness of the effect is supported by the fact that the spectra were recorded at 300 K. STM highlights the empty QWS, while Angle Resolved Photoelectron Spectroscopy [18] is better suited to detect the occupied QWS. First principle calculations of the band structure for isolated Pb(1 1 1) slabs [19] indicate that the QWS arise from $p_z$ states, and, thus, can be easily detected by STM. Similar results were also obtained for Pb nanocrystallites on Si(1 1 1) [20].

## 3. Magic heights and quantum well states

Fig. 3 reproduces the equilibrium height distribution of flat-top Pb(1 1 1) nanoislands grown on Cu(1 1 1), as obtained from STM images. The distribution shows the existence of "*magic*" heights, i.e. islands with certain heights appeared much more frequently than others in the equilibrium distribution [16]. Islands with magic height have also been observed during the growth of Pb on Si(1 1 1) 7 × 7 [21].

The magic heights are correlated to the *absence* of QWS close to the Fermi energy [16,21,18]. Calculations of the total energy (and surface energy) of the Pb film as a function of thickness relate the magic heights to *minima* in the energy of the Pb film [22,23]. The total energy of a thin metallic film oscillates with its thickness, in the case of Pb with quasi-bilayer periodicity. Since the periodicity (1.8 ML) is not exactly 2 ML, there is a beating pattern (9 ML) superimposed on the quasi-bilayer oscillations, similar to the supershell structure observed in nuclei and clusters, that produces an alternation of stable layers between odd and even numbers

[22,23]. The agreement of the predictions for 1D, jellium Pb films on Cu(1 1 1) [23] with the observed [16] magic heights for Pb/Cu(1 1 1) nanoislands is surprisingly good[1].

The QWS dictate the permitted heights of Pb crystallites by eliminating from the height distribution those nanocrystals whose heights would have an occupied QWS close to the Fermi level [16], and, thus, a large contribution of the electronic states to the total energy of the film. These observations can also be understood in the framework of the electronic growth model first introduced by Zhang [24] to explain the inverse Stranski-Krastanov mode of growth discovered for Ag on GaAs(1 1 0) [25], whereby a rough Ag film deposited at low temperature and consisting in nanoclusters, above a certain critical thickness (6 ML in that case) smoothes into a flat film (with voids) upon annealing.

## 4. Film stability and surface roughening

The surface roughening transition was introduced by Burton and Cabrera [26] more than fifty years ago in the framework of their classic theory of crystal growth. Below the roughening temperature, $T_R$, the surface of a crystal in equilibrium with its own vapor is atomically flat, while above $T_R$ it is rough (many heights are simultaneously exposed) because the free energy to create a step vanishes. The roughening temperature, operationally defined as the temperature of decomposition of every layer in favor of more stable heights, is proportional to the surface energy per atom, and, thus, any physical factor contributing to the surface energy will influence $T_R$. The roughening temperature has been shown experimentally to depend on the surface orientation for He [27] or Xe [28] crystals and also to be (monotonically) layer-dependent for thin films of Xe grown on Pd(1 1 1) [29,30]. In this latter case the population of the different layers as a function of T was deduced from the heights of the layer-dependent photoemission peaks [29].

Recently, the layer-dependent electronic energy contributed by QWS to the total energy of ultrathin metallic films with confined electrons has been shown to influence the thermal stability of ultrathin metallic films deposited on semiconducting [31,4,32] and metal substrates [33,34].

In order to explore the layer dependence of $T_R$ due to the oscillatory contribution of the QWS, atomically uniform films of Pb on Cu(1 1 1) have been prepared at low temperature (in contrast to the previous paragraph, in which Pb deposition was done with the substrate held at RT). Upon lowering the deposition temperature of Pb, the mode of growth changes to a layer-by-layer type, as atomic diffusion becomes progressively frozen. Below 100 K the growth occurs almost ideally layer-by-layer and the Pb films cover uniformly the substrate. Fig. 4 illustrates the morphology of a film of Pb 5.1 ML-thick deposited on Cu(1 1 1) at 98 K and kept this temperature. Only three levels are present at the surface upon deposition. Almost all the surface is covered with a film 5 ML-thick, but there are small regions imaged darker, corresponding to 4 ML, while the ramified, brighter, islands correspond to a local coverage of 6 ML.

Even if the films cover continuously the substrate, the exact local thickness of the deposited Pb films can be accurately determined experimentally by comparing the energy position of the corresponding QWS detected by Scanning Tunneling Spectroscopy with those observed on top of the Pb islands of various heights that appear upon deposition on Cu(1 1 1) at 300 K [16]. The inset of Fig. 4 shows the tunneling spectra recorded on top of the regions with local coverage of 5 and 6 ML. Notice that 6 ML (like all the thickness with an even number of atomic layers) presents a characteristic QWS at +0.65 eV [6,15].

[1] The Pb thickness as counted here includes the $(4 \times 4)$ wetting layer.

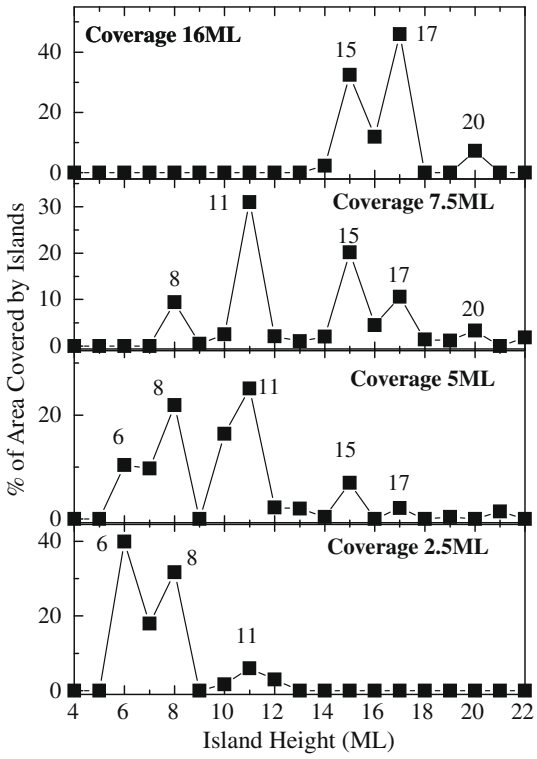


**Fig. 3.** Distribution of heights experimentally observed for Pb(1 1 1) islands deposited at 300 K on Cu(1 1 1). There are heights much more frequent than others and they are termed magic heights.

These experiments raise the question of why the QWS keep their energy position even very close to the interfaces between areas with different local thickness. The reason is that the QWS are well separated in energy, and thus, they can not easily mix. This

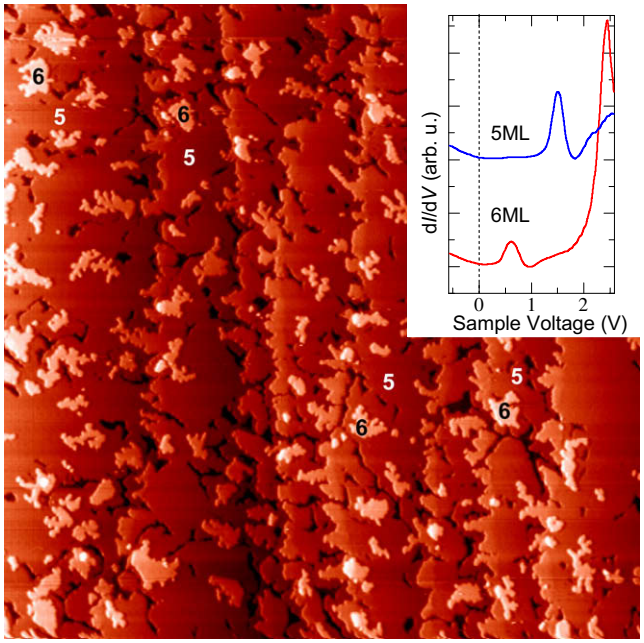


**Fig. 4.** 200 nm × 200 nm STM image recorded (sample voltage = −0.6 V, $I_t = 0.2$ nA) in situ after deposition of 5.1 ML of Pb on Cu(1 1 1) at 98 K. The inset shows tunnelling spectra recorded at 98 K on regions of the surface with local thicknesses of 5 and 6 ML of Pb. The tunnelling gap was stabilized at a sample voltage of −0.4 V and $I_t = 0.2$ nA. The spectra have been shifted vertically for clarity.

leads to their localization in the lateral direction, which allows their direct visualization in the real-space. To quantify this effect, *I–V* curves were recorded at each pixel of the STM images in order to construct spatial images of the current at different sample bias voltages in the −1.5 V to +2 V range. Some of them, corresponding to a 2.9 ML-thick film deposited and imaged at 98 K, are shown in Fig. 5. The regions with local thicknesses differing by one monolayer display QWS well separated in energy and, accordingly, they appear bright or dark as the corresponding QWS enter the energy window of the tunneling current images. The island at the lower left is bright at −1 V, while the one in the center is dark. Their relative contrast is inverted at +0.1 V, with the region at the upper left of intermediate brightness. At +0.8 V the relative contrast of upper and lower left regions have changed and at +2 V they reverse again as their corresponding QWS enter or exit the energy window.

STM at variable temperature can be used to follow the evolution of the morphology of the films during a quasi-static annealing with a temperature ramp of 1 K per minute. Fig. 6 shows large-scale STM images that illustrate the morphological changes observed in a 5 ML-thick Pb film as its temperature increases. The images during the annealing process have been recorded with the tip sufficiently far away from the substrate to minimize a possible influence of the tip electrical field in the observed mass transport. The film, is clearly rough at 220 K, and mostly 8 and 10 ML-high areas can be seen.

Films of different thicknesses have been grown at low temperature and their thermal stability determined by STM. From a large number of images, the fraction of surface area covered by each thickness has been evaluated and the roughening temperature corresponding to each layer obtained [34]. A summary of the roughening temperatures for each film is shown in the upper panel of Fig. 7. Each Pb layer becomes unstable at a different temperature and the roughening temperature oscillates with the thickness with bilayer periodicity. Films with a number of layers corresponding to the non-magic heights [15] (i.e. 2, 4, 5, 7 or 9 ML), which are flat at low temperatures because they are trapped by kinetic constraints, becomes rough and decompose into more stable heights (i.e. 6 and 8 ML-high islands) at lower temperatures. Pb films whose thickness correspond to magic heights (i.e. 3, 6, 8 or 10 ML) are stable to higher temperatures. The thermal stability of a film of $N$-layers thickness is proportional to the total energy of the film, $E(N)$, or to be more specific, a film is stable if $2E(N) < E(N-1) + E(N+1)$. The lower panel of Fig. 7 shows the calculated energy for isolated slabs of Pb(1 1 1) [22,23]. The minima in the calculated total energy of the system predict the relative stability of the different thicknesses. The calculated differences in surface energy are 10–20 meV/atom [22]. There is excellent agreement for most layer thicknesses, but there is a minor misplacement of the first beating. The disagreement is probably due to the fact that the reflection of

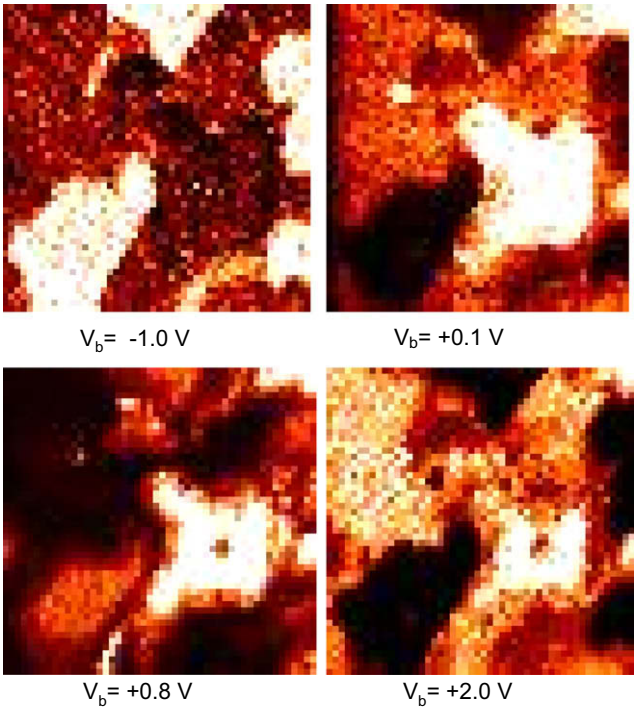


**Fig. 5.** 20 nm × 20 nm images of the spatial distribution of tunnelling current at specific bias voltages for a 2.9 ML-thick Pb film deposited and measured at 98 K on Cu(1 1 1). The color code reflects the tunnelling current al the bias voltages specified in each image.

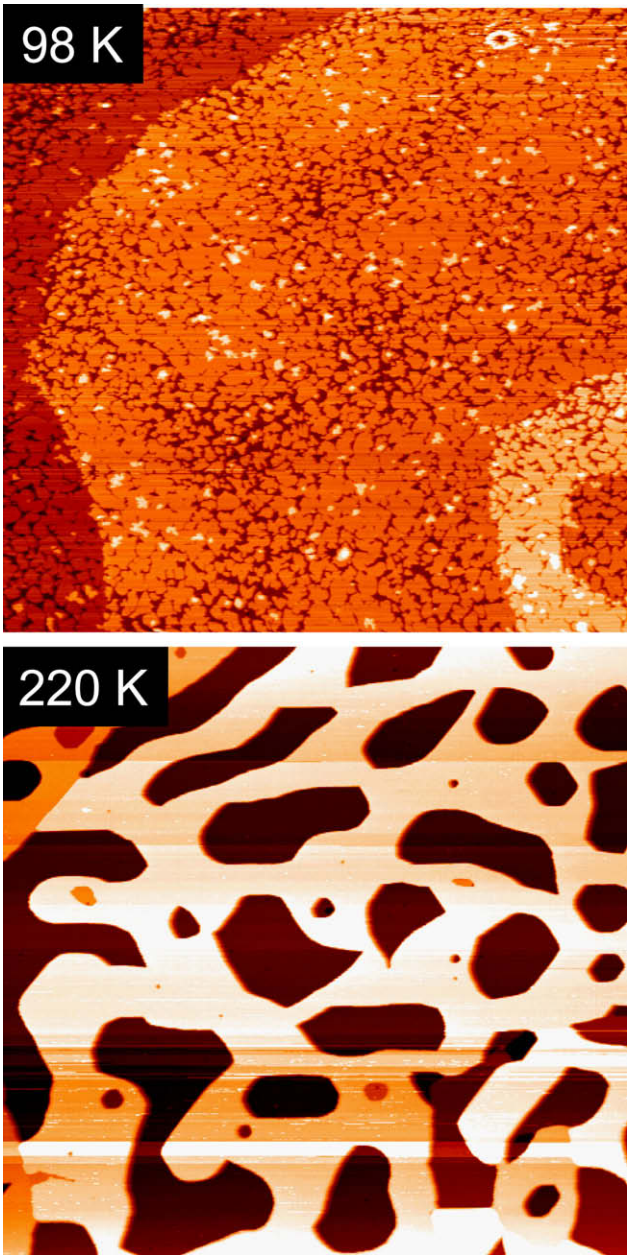


**Fig. 6.** 350 nm × 350 nm STM images recorded (sample voltage = −0.6 V, $I_t = 0.2$ nA) in situ after deposition of 5.1 ML of Pb on Cu(1 1 1) at 98 K (upper panel) and after heating to 220 K.

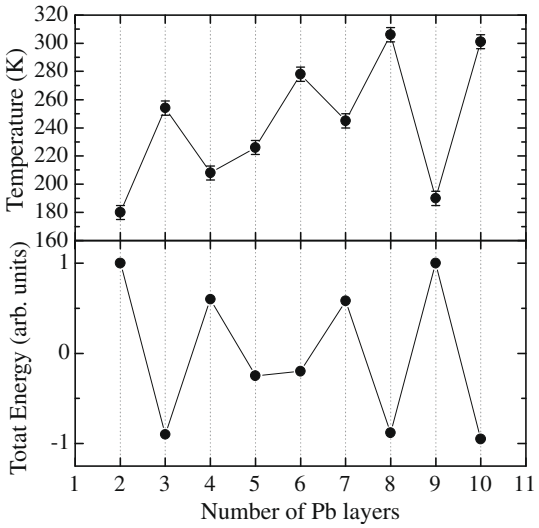


**Fig. 7.** The upper panel shows the roughening temperatures of the different layers as deduced from STM movies. The lower panel shows the calculated total energy of Pb(1 1 1) slabs as a function of thickness.

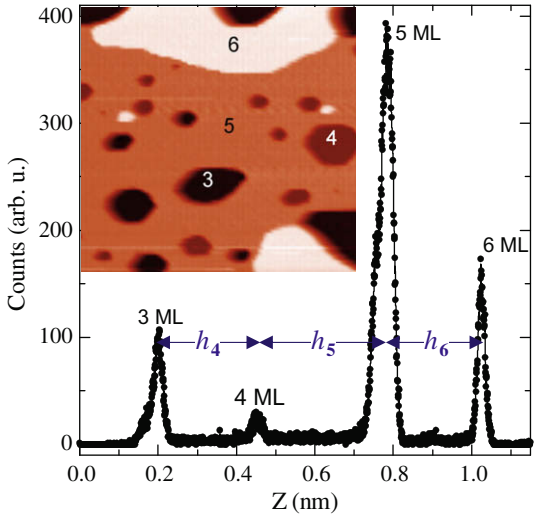


**Fig. 8.** The inset shows a 100 nm × 100 nm STM image of 5.1 ML-thick Pb film heated to 217 K ($V_b = -3$ V, $I_t = 0.08$ nA). The corresponding histogram of heights obtained after careful substraction of the plane in the STM images illustrates the procedure to determine the apparent step heights $h_N$.

electrons at the 4 × 4 Pb monolayer/Cu(1 1 1) interface, and, therefore, the phase shift of the oscillatory behavior, is not correctly described by the oversimplified model used in the calculations. First principle calculations by Wei and Chu [22] for free-standing Pb(1 1 1) slabs, predict the existence of the QWS at +0.65 eV for an even number of layers, which the jellium model does not, highlighting the role of the band structure in determining the energies of the QWS. For Pb/Si(1 1 1), both X-ray reflectivity [35] and STM measurements [32] indicate that 3–5 atomic levels are almost equally occupied for a film grown at low temperatures. The intensity of the QWS in Photoemission has been used to ascertain the degree of roughness of the Pb film upon annealing [31]. The population of the different layers has been deduced from fits to X-ray reflectivity measurements as a function of temperature [35]. The decomposition temperature of the Pb film depends on its number of layers. The maximum stability is observed for 6 and 8 ML-thick films, which are stable up to 250 K. No film of Pb has been reported so far to be stable up to room temperature. The $T_R$ values reported showed a single oscillation in the range of thicknesses explored [31], in general agreement with the data for Pb/Cu(1 1 1).

## 5. Apparent step heights

A role of QSE in crystal growth was first postulated to explain an apparent alternation of single and double layer growth detected by means of He scattering during the low temperature deposition of Pb on Cu(1 1 1) [36]. The effect was also related to an oscillatory behavior of the apparent step height deduced from He scattering [37]. The apparent step heights can directly be measured by STM as illustrated in Fig. 8 for an initially flat 5.1 ML-thick Pb(1 1 1) film. The film was thermally decomposed by applying a temperature ramp of 1 K/min, while STM images were continuously recorded in tunnelling conditions chosen not to disturb the morphology of the film by electric-field-induced mass transport [38] and to include the effects of the relevant occupied QWS. As we have seen, the initial morphology of the film changes upon increasing the temperature, since not all thicknesses are equally stable. The film roughens and new heights appeared in the images. The inset in Fig. 8 shows that, at 217 K, the percentage of the surface covered by a 5 ML-thick film has decreased (compare with Fig. 4), while layers of other thicknesses with lower total electronic energy, e.g. 3 or 6, increase their presence. Fig. 8 reproduces the particular histogram of heights corresponding to the image in the inset. From such histograms, the apparent step height for the *N*th layer, $h_N$, can be obtained. It is evident that $h_N$ is not constant. The measured step heights are independent of the tunneling conditions for negative sample biases, where the tunneling current from the occupied states reflects the DOS at the Fermi level. The values change strongly, however, for positive bias voltages, in particular, across the empty QWS in the +0.6 to +3 V range. Fig. 9 illustrates that the apparent step height measured by STM in a constant current topographic image, which results from scanning the tip over constant electron density contours in neighboring atomic terraces, contains both an *electronic* and a *geometric* contribution. The step height of layer $N$ is defined as $h_N = [t_N - t_{N-1}] + \left[\Delta^N_{vac} - \Delta^{N-1}_{vac}\right]$, where $t_N$ is the total thickness of a film with $N$ layers of Pb. $t_N = \sum_{i=1}^{N} d_i$, with $d_i$ being the different interlayer distances for a film N-monolayer thick. $\Delta^N_{vac}$ is the electron spillage length into the vacuum for a $N$-layer film, which depends on its electronic structure, in particular, on the DOS at the Fermi level. If $t_N$ increases linearly with $N$ and the electronic structure is independent of $N$, the apparent step height should be simply the bulk interlayer distance, i.e. $h_N = d_{bulk}$. This is what happens for bulk crystals, even when multilayer relaxations [39] are taken into account. If, however, either $t_N$ does *not* increase linearly with $N$, or $\Delta^N_{vac}$ depends on $N$ because of the QWS, $h_N$ will show a non-monotonous behavior. This is precisely the case at hand. Notice that for a film with an

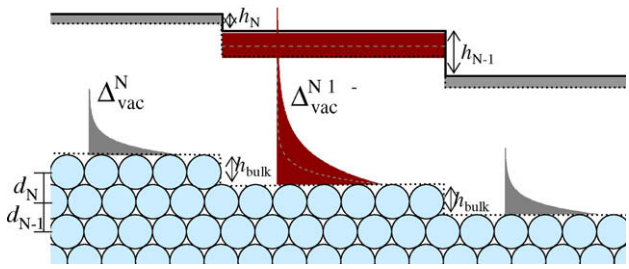


**Fig. 9.** (a) Schematic drawing of the origin of the thickness-dependent apparent step heights $h_N$ measured by STM. $\Delta^N_{vac}$ is the electron spillage length into the vacuum, which is controlled by the DOS at the Fermi level. $d_N$ is the interlayer distance.

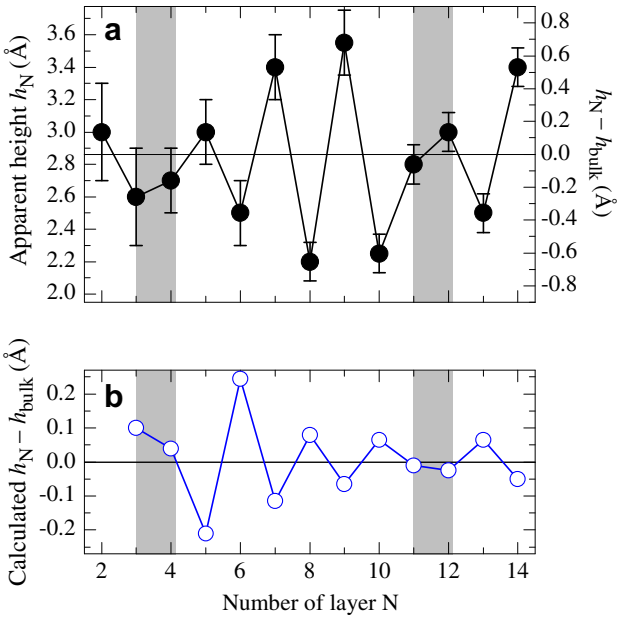


**Fig. 10.** (a) Apparent height differences, $h_N$, between Pb regions differing by a single atomic layer, as obtained from histograms in STM images (solid circles), such as Fig. 2. The horizontal line represents the Pb bulk interlayer distance at 200 K (2.84 Å). The gray areas mark phase slips in the observed bilayer periodicity. (b) Open circles are first-principles calculated differences in step height with respect to the bulk interlayer distance.

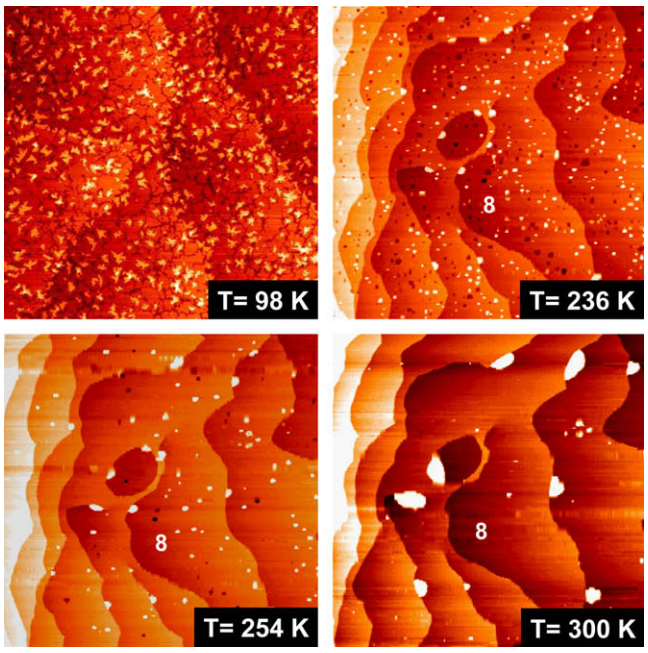


**Fig. 11.** 500 nm × 500 nm STM images at increasing temperatures for a 8 ML-thick Pb film deposited at 98 K on Cu(1 1 1).

occupied QWS close to the Fermi level, the DOS and the electron spillover, $\Delta_{vac}$, are larger and, accordingly, the apparent step height will be larger than the bulk interlayer distance. Fig. 10 shows that the apparent step height, $h_N$, (solid circles) for Pb(1 1 1) films grown on Cu(1 1 1) at 100 K *oscillates* with N, the number of Pb layers, around the ideal (1 1 1) interlayer distance in bulk Pb. Note that $N$ includes the $(4 \times 4)$ wetting layer. $h_N$ is clearly smaller than the bulk interlayer distance for $N = 3, 4, 6, 8, 10$ and 13 ML, and larger for $N = 2, 5, 7, 9$ and 12 ML. The oscillations have bilayer periodicity with a longer beating period that produces a phase slip every 8 ML. Five oscillations and two phase slips have been detected. The typical amplitude of the oscillation is 0.5 Å, but it reaches 1.2–1.4 Å for 7–10 ML. This observation is a clear indication that electronic effects are very important in this system. The apparent step height measured by STM reflects the different electronic structure of islands differing by just one atomic layer, in particular the different amount of charge spilling in the vacuum. The oscillatory behavior with bilayer periodicity is consistent with earlier observations of oscillations in the apparent step height deduced from He atom scattering during the growth of Pb films on Cu(1 1 1) at 140 K [37] or with STM [39] and XRD [4] observations for Pb on Si(1 1 1). Notice that since the QWS dominates the electronic structure of the film, the specific values of the apparent step height depend on the tunneling voltage used for imaging.

## 6. Quantum-stabilized mirror for atoms

As shown above, for a metallic film deposited on a substrate that confines efficiently the electrons, not all film heights are equally stable. Certain heights might be particularly stable, because the energy barriers to jump to the next stable height are larger. This can be exploited to stabilize at 300 K atomically flat films of Pb with specific heights, initially deposited at low temperatures. Fig. 11 illustrates the point for 8 ML-thick film of Pb/Cu(1 1 1). The film surface reproduces the steps of the substrate. The film can be heated to 300 K and still remains atomically flat, except for the regions around the step bunches of the substrate, where it decomposes slowly into 3D islands. The decomposition may often last many hours. Fig. 10 shows some selected snapshots from the movie corresponding to the heating of a Pb film 8 ML-thick. The upper image was recorded at 236 K, i.e. well above the decomposition temperature of the 9 ML film, and the film still shows only the 8th layer at the surface. In fact, the 8 ML Pb film is stable at 300 K except close to the step bunches of the substrate, a feature notably difficult to avoid in standard (1 1 1) fcc metallic single crystal substrates. When the Cu(1 1 1) substrate is prepared without

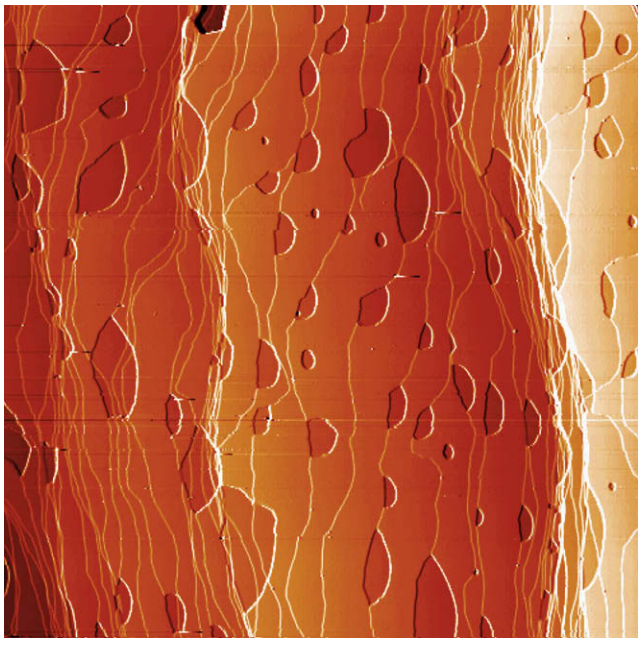

**Fig. 12.** 2000 nm × 2000 nm STM image of a 8 ML-thick Pb film deposited on Cu(1 1 1) at 98 K and heated to 300 K and kept there for 24 h. Most of the steps visible simply reflect those already present in the Cu substrate.

step bunches and the deposited coverage carefully adjusted to 8 ML, a metallic film atomically flat over lateral distances of microns can be stabilized at 300 K for days. Fig. 12 shows an 2 micron-wide STM image of a film of Pb deposited at low temperature, heated to and kept at 300 K (and imaged continuously) for more than 24 h. Only 1 ML-high atomic steps corresponding to the step height and density of the Cu substrate can be seen. This quantum-controlled, kinetic pathway to metastable, long-lived, ultrathin films can find applications in many different fields requiring atomically flat metallic films grown on semiconductor or insulators. It can also be used to fabricate a template of metallic wires of identical thickness [38]. In order to further improve the stability of the metallic film, a Si(1 1 1) crystal with a low density of steps have been used as a substrate. The resulting film of magic height do not show a single step in images that are 500 nm wide (Fig. 13). This has been used to fabricate a quantum-stabilized mirror for He atoms of unprecedented structural perfection composed of a film of magic height of Pb deposited on a 50 micron thick Si(1 1 1) wafer. It has been claimed that atomically uniform films of Pb on Si(1 1 1)have also been prepared at low temperature benefiting from the quantum confinement [31], but the lateral scale of the atomically flat regions was not reported.

## 7. Other magnitudes that oscillate with thickness

### 7.1. Oscillatory surface chemical reactivity

The chemical reactivity of a crystalline surface is known to depend on the crystallographic orientation, but since the DOS at the Fermi level is strongly affected by the energy location of the QWS in confined films, the surface reactivity is expected to oscillate with the thickness [40,41]. Indeed an oscillatory layer-dependent amount of adsorbed oxygen has been recently detected on Pb nanomesas grown on Si(1 1 1) [38]. This is in line with previous observations of layer-dependent oxidation of Mg thin films [40]. The difference in adsorption energy between adjacent layers has been estimated to be 9 meV [38]. Notice that this type of local experiment eliminates uncertainties associated to differences in exposure, but quantitative estimations of sticking coefficients are hard to extract from STM data. This, nevertheless, indicates that it might be possible to use metal films of different atomic thickness to deposit selectively certain molecules forming quantum-controlled nanostructures, such as organic wires.

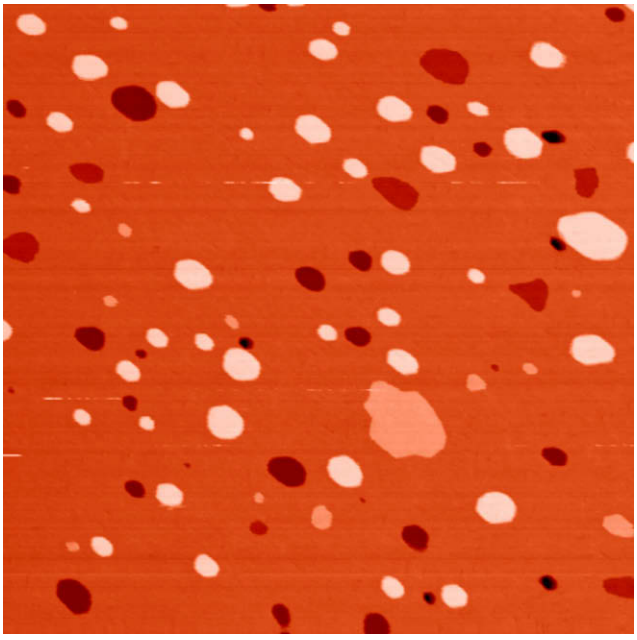

**Fig. 13.** 500 nm × 500 nm STM image of a 8 ML-thick Pb film deposited on Si(1 1 1) at 98 K and heated to 300 K. Notice that not a single step of the substrate is visible.

### 7.2. Layer-dependent surface diffusion

The kinetics of surface diffusion can also be affected by QSEs. Recently it has been found that the activation barrier for self-diffusion of Pb adatoms on the surface of ultrathin Pb films oscillates with the thickness of the underlying films [38]. For films of Pb on Si(1 1 1) the critical temperature of superconductivity [10,11] or the surface diffusion barrier [42] have been shown to oscillate, related to the QWS periodicity imposed by the Fermi surface of Pb.

### 7.3. Oscillatory work function

The average work function has been predicted to oscillate with the thickness [43,22]. The local tunneling barrier, which is related to the local work function, as given by PAX [44] has been shown to oscillate between 3.5 and 3.7 eV for Pb films deposited on Si(1 1 1). The local tunneling barrier tracks the energy position of the Highest Occupied QWS, i.e. it is larger when the HOQWS is far away from the Fermi level. These oscillations in the tunneling barrier enhance the oscillations of the apparent step height mentioned above.

## 8. Outlook

Pb islands grown in Cu(1 1 1) display quantized energy levels, known as Quantum Well States (QWS), that can be detected by STM. These QWS's play a decisive role to determine the structural and thermal stability of the Pb layers grown on Cu(1 1 1). At 300 K, Pb forms 3D nanostructures with magic heights, that correspond to islands having a QWS far from the Fermi energy. Below 100 K Pb grows in a quasi layer-by-layer fashion. The quantum well states that develop in the films determine their total energy and, accordingly, their thermal stability. Films of particularly magic thickness are stable upon heating to 300 K over lateral distances of microns, as visualized with STM. Financial support by the Ministerio de Ciencia e Innovación through projects FIS2007.61114 and CONSOLIDER on Molecular Nanoscience, and the Comunidad de Madrid, under grant NANOMAGNET S-0505/MAT-0194, is gratefully acknowledged.

## References

[1] V.B. Sandomirskii, Sov. Phys. JETP 25 (1967) 101.
[2] F. Schulte, Surf. Sci. 55 (1976) 427.
[3] P. Saalfrank, Surf. Sci. 274 (1992) 449.
[4] P. Czoschke, H. Hong, L. Basile, T.-C. Chiang, Phys. Rev. Lett. 91 (2003) 226801.
[5] J.-H. Cho, Q. Niu, Z. Zhang, Phys. Rev. Lett. 80 (1998) 3582.
[6] R.C. Jaklevic, J. Lambe, Phys. Rev. B 12 (1975) 4146.
[7] M. Jalochowski, E. Bauer, H. Koppe, G. Lilienkamp, Phys. Rev. B 45 (1992) 13607.
[8] M. Jalochowski, M. Hoffman, E. Bauer, Phys. Rev. Lett. 76 (1996) 4227.
[9] B.G. Orr, H.M. Jaeger, A.M. Goldman, Phys. Rev. Lett. 53 (1984) 2046.
[10] Y. Guo et al., Science 306 (2004) 1915.
[11] D. Eom et al., Phys. Rev. Lett. 96 (2006) 027005.
[12] Y.-F. Zhang et al., Phys. Rev. Lett. 95 (2005) 096802.
[13] A. Cebollada et al., Phys. Rev. B 39 (1989) 9726.
[14] M.N. Baibich et al., Phys. Rev. Lett. 61 (1988) 2472.
[15] R. Otero, A.L. Vázquez de Parga, R. Miranda, Surf. Sci. 447 (2000) 143.
[16] R. Otero, A.L. Vázquez de Parga, R. Miranda, Phys. Rev. B 55 (2002) 10791.
[17] J.E. Prieto, Ch. Rath, S. Müller, L. Hammer, K. Heinz, R. Miranda, Phys. Rev. B 62 (2000) 5144.
[18] J.H. Dil, J.W. Kim, S. Gokhale, M. Tallarida, K. Horn, Phys. Rev. B 70 (2004) 045405.
[19] Felix Lndurain, private communication.
[20] I.B. Altfeder, K.A. Matveev, D.M. Chen, Phys. Rev. Lett. 78 (1997) 2815.

[21] M. Hupalo, M.C. Tringides, Phys. Rev. B 65 (2002) 115406.
[22] C.M. Wei, M.Y. Chou, Phys. Rev. B 66 (2002) 233408.
[23] E. Ogando, N. Zavala, E. Chulkov, M.J. Puska, Phys. Rev. B 69 (2004) 153410.
[24] Z. Zhang, Q. Niu, Ch.-K. Shih, Phys. Rev. Lett. 80 (1998) 5381.
[25] A.R. Smith, K.-J. Chao, Q. Niu, Ch.-K. Shih, Science 273 (1996) 226.
[26] W.K. Burton, N. Cabrera, Disc. Faraday Soc. 5 (1949) 33.
[27] E. Avron et al., Phys. Rev. Lett. 45 (1980) 31;
E. Avron et al., Phys. Rev. Lett. 45 (1980) 814.
[28] R. Miranda, E.V. Albano, S. Daiser, G. Ertl, K. Wandelt, Phys. Rev. Lett. 51 (1983) 782.
[29] R. Miranda, E.V. Albano, S. Daiser, K. Wandelt, G. Ertl, J. Chem. Phys. 80 (1984) 931.
[30] J.M. Soler, N. García, R. Miranda, N. Cabrera, J.J. Saénz, Phys. Rev. Lett. 53 (1984) 822.
[31] M.H. Upton, C.M. Wei, M.Y. Chou, T. Miller, T.-C. Chiang, Phys. Rev. Lett. 93 (2004) 026802.
[32] M. Ozer, Y. Jia, B. Wu, Z. Zhang, H. Weitering, Phys. Rev. B 72 (2005) 113409.
[33] D.-A. Luh, T. Miller, J.J. Paggel, M.Y. Chou, T.-C. Chiang, Science 292 (2001) 1131.
[34] F. Calleja, M.C.G. Passegi Jr., J.J. Hinarejos, A.L. Vázquez de Parga, R. Miranda, Phys. Rev. Lett. 97 (2006) 186104.
[35] P. Czoschke, H. Hong, L. Basile, T.-C. Chiang, Phys. Rev. Lett. 93 (2004) 036103.
[36] B.J. Hinch, C. Koziol, J.P. Toennies, G. Zhang, Europhys. Lett. 10 (1989) 341.
[37] J. Braun, J.P. Toennies, Surf. Sci. 384 (1997) L858.
[38] C.-S. Jiang et al., Phys. Rev. Lett. 92 (2004) 106104.
[39] W.B. Su et al., Phys. Rev. Lett. 86 (2001) 5116.
[40] L. Aballe, A. Barinov, A. Locatelli, S. Heun, M. Kiskinova, Phys. Rev. Lett. 93 (2004) 196103.
[41] A.G. Danese, F.G. Curti, R.A. Bartynski, Phys. Rev. B 70 (2004) 165420.
[42] T.L. Chen et al., Phys. Rev. Lett. 96 (2006) 226102.
[43] C. Marliere, Vacuum 41 (1990) 1192.
[44] K. Wandelt, J. Vac. Sci. Technol. A 2 (1984) 802.